ON THE IMPORTANCE OF SOLID DEFORMATIONS IN CONVECTION-DOMINATED LIQUID/SOLID PHASE CHANGE OF PURE MATERIALS*

Daniela Mansutti, Roma, Edoardo Bucchignani, Capua

Cordially dedicated to Professor K. R. Rajagopal on the occasion of his sixtieth anniversary, with particular sincere gratefulness from D. M. for his precious support and continuous guidance

Abstract. We analyse the effect of the mechanical response of the solid phase during liquid/solid phase change by numerical simulation of a benchmark test based on the well-known and debated experiment of melting of a pure gallium slab counducted by Gau & Viskanta in 1986. The adopted mathematical model includes the description of the melt flow and of the solid phase deformations. Surprisingly the conclusion reached is that, even in this case of pure material, the contribution of the solid phase to the balance of the momentum of the system influences significantly the numerical solution and is necessary in order to get a better match with the experimental observations. Here an up-to-date list of the most meaningful mathematical models and numerical simulations of this test is discussed and the need is shown of an accurate revision of the numerical simulations of melting/solidification processes of pure materials (e.g. artificial crystal growth) produced in the last thirty years and not accounting for the solid phase mechanics.

Keywords: liquid/solid phase change, deformation, convection, numerical simulation, finite differences

MSC 2010: 80A22, 35R37, 35Q99, 78M20

1. Introduction

Solidification and melting are associated with many practical applications, ranging from industrial processes to environmental engineering, so that their proper understanding is not only of scientific interest; just to mention few applications, they are

relevant to industry for artificial crystal production and metal casting, to planetology for studying the evolution of the crust of icy planets, to ecology for forecasting the perennial glacier melting, and to energy production for preventing crystal formation in the cooling system of energy storage apparata (space stations, nuclear power plants). In the sequel we go, briefly, through the main steps of recent research devoted to the description and understanding of the mechanisms of liquid/solid (L/S) phase transitions.

The first fundamental approach to mathematical modelling was due to Stefan [49] who studied the melting of the ice polar cap and started the fortune of the "Stefan model". Afterwards, numerous and more general models have been produced for the description of general L/S phase transition processes, that take into account different thermodynamical mechanisms more and more detailed [12]. In the seventies, experimentalists started to characterize the influence of dynamics: in 1970 Szekeley & Chambra [50] were probably the first to provide quantitative evidence (through experiment and analytical results) of the effect of melt natural convection on the phase front shape by operating in a rectangular cavity with heat source and sink on the two opposite vertical walls. In 1977, Chiesa & Guthie [10] and, seven years later, Gau & Viskanta [22] shew experimentally that melt convection reduces (increases) the rate of solidification (melting) of a metal. Finally, in 1986, with the well-known experiment of melting (solidification) of a pure gallium slab heated (cooled) from a vertical side [23], Gau & Viskanta definitely confirmed the importance of natural convection even in this case of low Prandtl material. Then, the analysis of the mechanisms of solidifying/melting systems, both via experimental work and via numerical simulation, has been especially focused on the characterization of the fluid dynamics of the melt and its effects on the process [20], and, in most cases, the processes have been classified as convection dominated ones [33].

In literature, works on pure materials appeared first. The paper by Hurle [32] deals with the transitions of the horizontal convective flow of the melt in artificial crystal growth systems. On this issue a bunch of papers have been published throughout the following years to nowadays (e.g., more recently, Viswanath & Jaluria [55], De Groh III & Lindstrom [16], Rady & Mohanty [44], Voller [57], Yeoh et al. [58], Chen et al. [9], Bertrand et al. [5], Sampath & Zabaras [45], Bansch & Smith [4], Kim et al. [35]). The applicative interest in this specific matter is due to the fact that oscillatory instabilities in the melt flow are one of the main causes of the appearance of dishomogeneities and defects in the final crystal. Actually the solidifying material is usually mixed to solutes, added in order to diminish the melting temperature and to slow down the process for easier control; but oscillatory melt motion induces non uniform distribution of such substances and, consequently, non uniform phase change. So these studies were aimed at providing the knowledge how to drive the

118

growth technique in order to avoid oscillations in the melt and build improved crystals without dishomogeneities. The mathematical models typically adopted were based on the classical heat balance equation for the whole system, melt and solid phases, combined with the momentum balance equation for the melt.

When the material is non-euthectic (e.g. alloys), the interaction between the melt and the growing (or shrinking) solid, while phase transition takes place, is very strong through the rigid dendrites or the granules of the mush, that is the characteristic intermediate phase [8].

In fact, it appears that such interaction is effective also in the case of euthectic materials according to what has been found via X-ray measurements during experiments of melting of pure metals (Gondi et al. [25], Costanza et al. [11]): structural variations in the solid portion close to the phase interface have been observed and may be correlated to the melt convection. Mathematical and numerical assessments have been, however, invoked by the authors as the measured physical quantities are very small and might have been spoiled by experimental errors. The present work is to be inserted at this point of the research landscape of this field as it contributes to shed light upon the mechanisms accompanying a pure material L/S phase change.

The following overview of mathematical models, typically built for the simulation of non-euthectic materials, might be assumed, then, to provide hints also for the treatment of euthectic materials. Such models designed for studying the combined effect of the dynamics of the liquid and of the solid phases, can be grouped into enthalpy models, granular models and multiphysics models. For the description of the energy conservation of the system, the enthalpy models introduce the total enthalpy, including with sensible heat the amount of latent heat *absorbed from/released to* the environment during melting/solidification; in addition, the dynamics of melt, mush and solid phases is described through a single momentum equation, by either the porous medium model or the viscoplastic model or a parametrical combination of models. In the first case liquid and solid phases are included as limit cases respectively with null and infinite porosity coefficients (see, for example, Voller et al. [56], Lamazouade et al. [37], Stella & Giangi [48] and Kang & Ryou [34]); in the second case liquid, solid and mushy phases are represented within a temperature dependent viscoplastic model (Song et al. [47]), whereas, in the third case, the three phases contribute parametrically to the momentum balance as a viscous fluid, a porous medium and a Hooke's thermoelastic material (Teskeredzic et al. [52]). In each of the models a unique equation for the whole system holds for each pertaining conservation law (momentum, mass and energy), so that the explicit moving boundary (phase front) computation is avoided. This is the case also for the model proposed by Hills and Roberts in the 90's that describes a liquid/solid phase changing system as a binary "reacting" granular mixture relaxing toward a state of local thermodynamic

119

equilibrium with the phases at the same interfacial pressure [28]. About ten years later this idea has been embedded by De Fabritiis et al. [15] and by Miller et al. [43] into the formalism of the thermal lattice Boltzmann method; they included a "reaction" mechanism enhanced by the thermal field as soon as the critical temperature is reached; the parallelism with the chemical "reaction" recovers the absorption/release of heat according to the characteristic latent heat, typical of the process.

The above mentioned "fixed grid" (enthalpic and granular) models provide easily phase fronts of any shape. However, when they are reduced for euthectic materials (no mush forming), an accurate numerical solution requires *a priori* very fine discretization meshes, due to the fact that the phase front is detected as a region, and not as a line, and requires necessarily at least one discretization cell wide.

Finally, multiphysics models describe the solidification/melting processes by representing the multiple mechanisms involved through separate equations in each phase. This approach then allows to treat each aspect with the necessary numerical resolution and *ad hoc* numerical tools overcoming the limitation of the previous set of models. The challenge, here, is to match the numerical variables typically computed upon different scales, a procedure that requires specific care in order to avoid additional inaccuracies. Bailey et al. in [2] adopted multiphysics modelling for studying metal casting and Cross et al. in [13] extended the model also to metal electromagnetic melting processes.

Among the models and papers mentioned so far the ones by Teskeredzic et al. [52] have to be pointed out as, although without any explicit justification, the authors adopted an enthalpic model with a thermoelastic solid phase also for the simulation of melting and solidification of pure materials. This choice is not at all obvious because several characteristics of the phase change processes, that are response to solid phase mechanics (e.g. bubble formation), are indeed absent in pure materials, so that solid mechanics seems to be negligible. In fact, in the present work we show definitely that it is not true.

We approach the numerical simulation of L/S phase transitions by a multiphysics mathematical model that, beside melt dynamics, heat transport phenomena and evolution of the phase front, provides also the description of the solid phase motion (Baldoni [3]). As in any real occurrence of L/S phase change, the prognostic variables considered are the velocity of the process, the shape of the interface and the value of the stresses between the phases. Here, we shall see how much solid phase mechanics affects such quantities by developing the numerical simulation of the experiment by Gau & Viskanta [23] (melting from a side of a pure gallium slab). This experiment is particularly suitable to this purpose as it has been numerically simulated, without solid dynamics, by many specialists in the literature of the recent past years and both the mechanisms of the physical process and the details of the mathematical and

120

numerical modelling have been deeply analysed, although some exciting elements of discussion are still left.

This paper is organized as follows: the mathematical model is presented in Section 2, the description of the Gau & Viskanta experiment is provided in Section 3, the numerical solution technique is sketched in Section 4, the numerical results are discussed versus the experimental observations in Section 5 and conclusions are drawn in Section 6.

2. The mathematical model of L/S phase change

The equations that govern the evolution of a continuum sample undergoing L/S phase transition have to include the representation of the conservation laws of momentum, of energy and of mass; for their structure we refer to the books on classical mechanics (e.g. [46]). A set of equations for each single phase is obtained together with the *jump conditions* for the balance of momentum, energy and mass across the phase interface. In the jump condition for the energy conservation law (the so called *Stefan condition* [12]), the most important is the contribution due to the release or the adsorption of latent heat corresponding respectively to the solidification or the melting processes.

In the model adopted here the liquid phase and the solid phase are described respectively as an *incompressible viscous fluid* [53] and an *isotropic linearly elastic incompressible material* [31], [30]. This choice allows to keep at average the level of difficulty of the final system of equations to be solved. Obviously, for the solid, a more appropriate model would be the one describing correctly the specific material symmetry but, here, we aim at providing a first insight into the effects of the mechanical response of the solid within the transition process. Additional simplifying assumptions are:

  i) the densities of the liquid and solid phases are constant and their difference is negligible; moreover, the Boussinesq-Oberbeck approximation applies in order to account for the buoyancy force,
 ii) the radiating heat is negligible,
iii) liquid and solid interfacing particles do not slip over each other,
 iv) the material coefficients of the two phases are constant and the thermophysical properties are the same.

The Boussinesq-Oberbeck approximation [19], mentioned in i), allows just (linear) density changes due to temperature variations to support the buoyancy effects; these are particularly important in our study case, the Gau & Viskanta experiment in [23], as they include also the convective motions. All the above assumptions have been

121

diffusely adopted in the published numerical simulations of this experiment referred in the present work; in the next section, we shall discuss their feasibility in the specific experimental context.

If t is the time and (x, y) the space cartesian coordinates, let us denote by D_L, D_S and $\Gamma(t)$ the domains occupied respectively by the melt, the solid and the phase interface. Supposing that heat conduction follows the classical Fourier's law, the governing equations of the melt flow, holding in D_L, read

$$(2.1) \qquad \varrho \frac{d\mathbf{v}_L}{dt} = -\nabla p_L + \mu_L \nabla^2 \mathbf{v}_L - \varrho[1 - \alpha(T_L - T_p)]\mathbf{g},$$

$$(2.2) \qquad \nabla \cdot \mathbf{v}_L = 0,$$

$$(2.3) \qquad \varrho c \frac{dT_L}{dt} = k\nabla^2 T_L + \mu_L \Big[\Big(\frac{\partial u}{\partial x}\Big)^2 + \frac{1}{2}\Big(\frac{\partial u}{\partial y} + \frac{\partial v}{\partial x}\Big)^2 + \Big(\frac{\partial v}{\partial y}\Big)^2 \Big]$$

with $\mathbf{v}_L = (u, v)$, p_L, T_L and ϱ respectively the velocity, the pressure, and the temperature of the melt, and with ϱ the density of the sample at the the reference temperature T_p (here, chosen to be coincident to the initial temperature). These equations are coupled with the following ones for the solid phase holding in D_S:

$$(2.4) \qquad \varrho \frac{\partial^2 \mathbf{U}}{\partial t^2} = -\nabla p_S + \mu_S \nabla^2 \mathbf{U} - \varrho[1 - \alpha(T_S - T_p)]\mathbf{g},$$

$$(2.5) \qquad \nabla \cdot \mathbf{U} = 0,$$

$$(2.6) \qquad \varrho c \frac{\partial T_S}{\partial t} = k\nabla^2 T_S,$$

with $\mathbf{U} = (U_x, U_y)$, p_S and T_S respectively the displacement, the (indetermined) pressure and the temperature of the solid phase. The symbols c, k and α indicate respectively the specific heat, the conductivity and the thermal expansion coefficients for the whole sample, whereas μ_L and μ_S are the viscosity coefficient of the melt and the second Lamé constant of the solid. Taking into account that $\mathbf{v}_L$ and $\mathbf{U}$ are solenoidal, the jump conditions, holding in $\Gamma(t)$, are

$$(2.7) \qquad \mathbf{v}_L = \mathbf{v}_S,$$

$$(2.8) \qquad (-p_L \mathbf{I} + \mu_L(\nabla \mathbf{v}_L + (\nabla \mathbf{v}_L)^T)) \cdot \hat{\mathbf{n}} = (-p_S \mathbf{I} + \mu_S(\nabla \mathbf{U} + (\nabla \mathbf{U})^T)) \cdot \hat{\mathbf{n}},$$

$$(2.9) \qquad -\varrho\Lambda(\mathbf{v}_L \cdot \hat{\mathbf{n}} - u_{\mathbf{n}}) - k\nabla T_S \cdot \hat{\mathbf{n}} + k\nabla T_L \cdot \hat{\mathbf{n}} = 0$$

with $\mathbf{v}_S$ the solid velocity computed from $\mathbf{U}$, $\hat{\mathbf{n}}$ the normal unitary vector on $\Gamma(t)$, Λ the latent heat and $u_{\mathbf{n}}$ the normal speed of the interface. The set of equations (2.1)–(2.9) is completed by initial and boundary conditions according to the known requirements of the classical fluid and solid mechanics models [46]. We focus on the fact that, at the phase front, the classical no-slip condition, which holds for viscous fluids

122

on a rigid wall, is replaced by (2.7) that expresses the fact that the interfacing fluid and solid particles are compelled to move sticking to each other at the same velocity. On the contrary, in models for L/S phase change that neglect the solid deformations, the no-slip condition implies that the fluid particles at the phase front have null velocity.

This model has already provided numerical results in agreement with the analytical solution in the case of the solidification of a semi-infinite water layer [41]. In the case of two-dimensional applications, by observing that the vectors $\mathbf{v}_L$ and $\mathbf{U}$ are both required to be solenoidal, we have obtained a reformulation of the model on the basis of the Helmoltz-Hodge decomposition in order to meet more accurately and easily such constrain. The theorems supporting this decomposition are recalled below in the three-dimensional more general case [1]:

Theorem 1. *Assume D is a closed set in $\mathbb{R}^3$ with ∂D continuously differentiable. Then for every $\mathbf{q} \in [C^2(D)]^3$ can be decomposed as a sum of a gradient of a scalar field $p \in C^3(D)$ (the so called scalar potential) and a solenoidal vector $\mathbf{u} \in [C^2(D)]^3$ parallel to ∂D:*

$$\mathbf{q} = \nabla p + \mathbf{u}.$$

Theorem 2. *Assume D is a closed simply connected set in $\mathbb{R}^3$ with ∂D continuously differentiable. Then, for $\mathbf{q} \in [C^2(D)]^3$, there is a vector field $\psi \in [C^3(D)]^3$ (the so called vector potential) such that*

$$\mathbf{q} = \nabla \times \psi$$

if and only if $\mathbf{q}$ is divergence-free.

The procedure is well known and experimented for the numerical simulation of incompressible flows [40] and, in the two-dimensional case, leads to the scalar potential/streamfunction/vorticity (φ, ψ, ω) formulation [29] through the following relations with the primitive variables (here referred to the melt flow nomenclature):

$$(2.10) \qquad \mathbf{v}_L = \nabla \varphi + \nabla \times \psi_L = \left(\frac{\partial \varphi}{\partial x} + \frac{\partial \psi_L}{\partial y}, \frac{\partial \varphi}{\partial y} - \frac{\partial \psi_L}{\partial x} \right),$$

$$(2.11) \qquad \omega_L = \frac{\partial v}{\partial x} - \frac{\partial u}{\partial y}.$$

In [42] we have extended this approach also to the treatment of the solid phase equations. As non-homogeneous Dirichlet boundary conditions on the normal component

123

of $\mathbf{U}$ are not expected, only streamfunction-like, ψ_S, and vorticity-like, ω_S, are required as new unknowns (see Theorem 1); they are linked to $\mathbf{U}$ through the following relations:

$$(2.12) \qquad \mathbf{U} = \nabla \times \psi_S = \left(\frac{\partial \psi_S}{\partial y}, -\frac{\partial \psi_S}{\partial x} \right),$$

$$(2.13) \qquad \omega_S = \frac{\partial U_y}{\partial x} - \frac{\partial U_x}{\partial y}.$$

By adopting the expressions (2.10), (2.11), (2.12), and (2.13) and applying the curl operator to the vector equations (2.1) and (2.4), the scalar equations for ω_L and ω_S are obtained; ψ_L and ψ_S result from the Poisson equations derived from the definition of ω_L and ω_S, whereas φ comes from the Laplace equation corresponding to the incompressibility constrain on $\mathbf{v}_L$. Finally, in the new formulation, the governing equations for the liquid phase are

$$(2.14) \qquad \varrho \frac{d\omega_L}{dt} = \mu_L \nabla^2 \omega_L - \varrho \alpha g \frac{\partial T_L}{\partial x},$$

$$(2.15) \qquad \nabla^2 \varphi = 0,$$

$$(2.16) \qquad \nabla^2 \psi_L = -\omega_L,$$

$$(2.17) \qquad \varrho c \frac{dT_L}{dt} = k\nabla^2 T_L + \mu_L \left[\left(\frac{\partial^2 \psi_L}{\partial x \partial y} + \frac{\partial^2 \varphi}{\partial x^2} \right)^2 \right.$$
$$\left. + \frac{1}{2} \left(\frac{\partial^2 \psi_L}{\partial y^2} - \frac{\partial^2 \psi_L}{\partial x^2} + 2\frac{\partial^2 \varphi}{\partial x \partial y} \right)^2 + \left(-\frac{\partial^2 \psi_L}{\partial x \partial y} + \frac{\partial^2 \varphi}{\partial y^2} \right)^2 \right],$$

while, for the solid phase, the governing equations are

$$(2.18) \qquad \varrho \frac{\partial^2 \omega_S}{\partial t^2} = \mu_S \nabla^2 \omega_S + \varrho \alpha g \frac{\partial T_S}{\partial x},$$

$$(2.19) \qquad \nabla^2 \psi_S = -\omega_S,$$

$$(2.20) \qquad \varrho c \frac{\partial T_S}{\partial t} = k\nabla^2 T_S.$$

It is worth noticing that in the transformed momentum equations, (2.14), and (2.18), the gradient of pressure is cancelled by the curl operator so that pressure is no longer in the unknowns list. In the jump conditions (2.7)–(2.9), the expressions (2.10), (2.11), (2.12), and (2.13) are also to be taken into account; in addition, the jump condition (2.8) is transformed via the application of the curl operator to the left and right momentum equations. Initial and boundary conditions for the new systems are computed in terms of the derived variables by substitution of the primitive initial and boundary values into the relating expressions.

124

We stress that the reformulation adopted, whatever the accuracy of the numerical computation of ψ_{S} is, yields a numerical displacement field $\mathbf{U}$ that, due to the decomposition (2.12), meets automatically the equation for mass conservation (2.5). Also in the melt, solenoidality of the numerical velocity field $\mathbf{v}_{\mathrm{L}}$ is much more easily recovered through the solution of the intensively studied Laplace equation (2.15) rather than with some tricky algorithm for the evaluation of pressure that, now, does not need to be computed. Another appreciable advantage of the adopted reformulation is the reduction of the number of PDEs of the whole final system from eight to six equations (the gain is, obviously, more evident in the three-dimensional case).

3. The Gau & Viskanta experiment

The experiment simulated here is the melting of a gallium slab heated on a side presented in [23]. Initially the gallium sample has a rectangular shape and is confined in a rigid cavity whose horizontal walls are adiabatic (dimensions of the layer, $8.89\,\mathrm{cm} \times 6.35\,\mathrm{cm}$). The initial temperature is $T_p = 28\,^{\circ}\mathrm{C}$, below the melting temperature that is $T_m = 29.78\,^{\circ}\mathrm{C}$. Suddenly a vertical wall, let us say the left one, is superheated at temperature $T_H = 38\,^{\circ}\mathrm{C}$ while the vertical wall at the right side is kept at $T_{\mathrm{S}} = T_p$ in order to induce the melting process in a unidirectional way. As Gau & Viskanta [23] and Brent et al. [6] noticed, the melting process is mainly governed by the heat transfer in the liquid strip, so the physical properties of the liquid phase, rather than those of the solid phase, dominate the phase change process. Moreover, the range of temperature used by the experimentalists is quite narrow ($10\,^{\circ}\mathrm{C}$) and, also, the melt flow has an averaging effect so that the assumption (in the previous section at iv)) of constant material coefficients and thermo-physical properties (made at iv) in the previous section) appears indeed reasonable. In agreement with these observations, in our simulation test, the values of density, volumetric thermal expansion, thermal conductivity and specific heat are assumed equal to those of the liquid phase (at $32\,^{\circ}\mathrm{C}$) throughout the two phases, that is, respectively, $\varrho = 6093\,\mathrm{kg} \cdot \mathrm{m}^{-3}$, $\alpha = 1.2 \times 10^{-4}\,\mathrm{K}^{-1}$, $k = 32\,\mathrm{W} \cdot \mathrm{m}^{-1} \cdot \mathrm{K}^{-1}$ and $c = 381.5\,\mathrm{J} \cdot \mathrm{kg}^{-1} \cdot \mathrm{K}^{-1}$. In a solidification process, the highly anisotropic behaviour of the polycrystalline gallium could not have been ignored and assumption iv) could not have been made.

As indicated in [23], other physical parameters of interest in the experiment have the following values: dynamic viscosity of the melt $\mu_{\mathrm{L}} = 1.81 \times 10^{-3}\,\mathrm{kg} \cdot \mathrm{m}^{-1} \cdot \mathrm{s}^{-1}$ and latent heat of fusion $\Lambda = 80160\,\mathrm{J} \cdot \mathrm{kg}^{-1}$; the second Lamé constant of the solid phase is assumed to be $\mu_{\mathrm{S}} = 10\,\mathrm{GPa}$.

4. NUMERICAL SOLUTION PROCEDURE

We approach the solution of the PDE model in Section 2 via a finite difference method based on the first order Euler scheme for first order time derivatives, the second order backward scheme for second order time derivatives, and centred second order schemes for space derivatives. In doing so, the unknowns, ω_L, ω_S, T_L, and T_S, result explicitly determined from the discrete form of the evolutive equations within a time marching algorithm. The Laplace equation for the scalar potential and the Poisson equations for the stream-functions are solved by a Bi-CGStab method [54], supported by a pre-conditioner based on the ILU factorization [24].

A fundamental aspect of our solution procedure consists in the application of a front-fixing technique [12] that overcomes the difficulties related to the moving boundary formulation: for each phase, a coordinate transformation is adopted in order to transform the time dependent spatial domains, D_L and D_S, into the unitary square and make the finite difference discretization straightforward. Obviously, such transformations generate new factors to the differential operators of the model which depend on the function of the unknown curve of the phase front. At each time step the discrete points of this curve are properly advanced according to the value of $u_\mathbf{n}$, the normal speed of the front, computed by the Stefan condition.

We stress that at the initial time $t = 0\,\mathrm{s}$, in order to start the numerical computation we needed to introduce as a numerical artifact the existence of a melt strip that we chose to be 0.1 cm thick.

In this paper we do not want to devote more space to the description of the numerical method as it is standard although supported by a good know-how in computing techniques, indispensable for the accomplishment of this very lengthy simulation (this aspect is confirmed by the other researchers that challenged themselves in this task, e.g. Stella & Giangi [48]). We rather want to draw the attention of the reader to our numerical results and their innovative impact in the literature on the simulations of the Gau & Viskanta experiment and even on the mathematical numerical modelling of L/S phase change.

Those who have simulated this experiment know that it is highly desirable to keep the number of discrete unknowns as low as possible and to use time steps as large as possible in order to cope with the long computing time required to cover the 19 min of experimental observation time. In our case the space discretization grid used for the results that will be presented shortly is 17×60 both in D_L and in D_S, and the larger time step allowed by numerical stability constrain was $\Delta t = 10^{-6}\,\mathrm{s}$.

For the severe time step limitation, certainly, the explicit schemes for momentum and energy equations are mostly responsible but also the intrinsic nonlinear nature of a moving boundary model comes into play in this matter. About the choice

126

www.r

of the space mesh, it is supported by mesh refinement analysis whose results are summarized in the drawing in Fig. 1, where the melt horizontal velocity profiles at
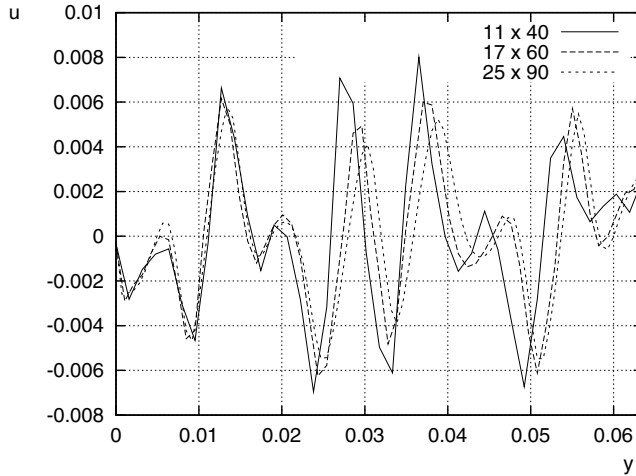

Figure 1. Melt horizontal velocity profiles at $x = 0.57$ cm (about the middle of the recirculation cell) computed at $t = 32$ s on progressively refined meshes (m and m/s are respectively the measure units over (x) and (y) axes).

the abscissa $x = 0.57$ cm and at time $t = 32$ s are shown for three different space meshes (11×40, 17×60, and 25×90). Though such profiles are not sufficient to state convergence, we rely on them as they are very close to the corresponding ones computed by Stella & Giangi in [48] with finer space grids. In Tab. 1 we also list the maximum and minimum values of ψ, u and v for each tested mesh on the whole domain. From the values of ψ it seems that the overall method is second order accurate in space. The small differences registered between the values on the grids 17×60 and 25×90 guarantee that the solution on the coarser one is accurate enough for our purposes. It is worth noting that the relative errors of u and v are generally higher than that of ψ according to expectations as u and v are derived quantities in the $\varphi/\psi_{\mathrm{L}}$ decomposition.

	$\mathbf{11 \times 40}$	$\mathbf{17 \times 60}$	$\mathbf{25 \times 90}$
$\psi_{\max}$	$7.551 \cdot 10^{-3}$	$3.982 \cdot 10^{-2}$	$2.760 \cdot 10^{-2}$
$\psi_{\min}$	-1.893	-1.631	-1.577
$\mathbf{u}_{\max}$	$8.168 \cdot 10^{-3}$	$6.159 \cdot 10^{-3}$	$5.788 \cdot 10^{-3}$
$\mathbf{u}_{\min}$	$-7.105 \cdot 10^{-3}$	$-6.284 \cdot 10^{-3}$	$-5.698 \cdot 10^{-3}$
$\mathbf{v}_{\max}$	$3.946 \cdot 10^{-2}$	$2.899 \cdot 10^{-2}$	$2.024 \cdot 10^{-2}$
$\mathbf{v}_{\min}$	$-1.246 \cdot 10^{-3}$	$-1.283 \cdot 10^{-3}$	$-1.300 \cdot 10^{-3}$

Table 1. Mesh sensitivity analysis at $t = 32$ s: maximum value and minimum value of ψ (in m^2/s), u and v (in m/s) on the whole domain.

www.r

Let us draw now the attention to Fig. 2, the plot of the computed phase fronts at the observation times reported by Gau & Viskanta, nine profiles from $t = 2$ min up to
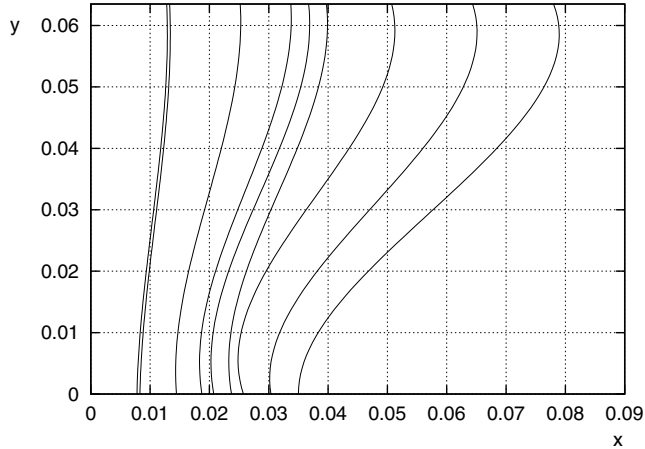

Figure 2. **Simulated** L/S phase fronts (solid mechanics *included* in the modeling) at the observation time instants of the experiment (m is the measure unit over (x) and (y) axes).

$t = 19$ min. The shape of the interface is initially a vertical line in accordance with the uniform heating of the left vertical wall, then it becomes more and more curved due to the convective motion of the melt induced by the horizontal temperature gradient. The plot in Fig. 2 has to be compared with the one in Fig. 3 (redrawn from Gau &
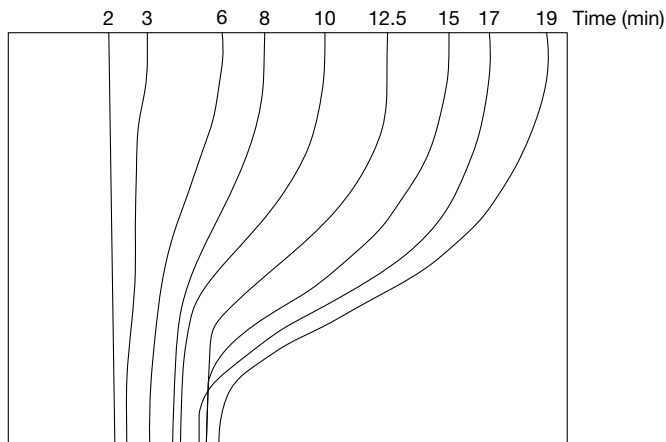
Figure 3. **Experimental** L/S phase fronts traced by Gau & Viskanta at preselected times (C. Gau and R. Viskanta, Melting and solidification of a pure metal on a vertical wall, Transaction of the ASME *108* (1986), 174–181).

Viskanta's plot at Fig. 2 (a) in [23]), where the corresponding experimental profiles are drawn. In comparison with numerical simulations in literature, which will be recalled and discussed in the next section, we report here a very good agreement, both in terms of the shape of the profiles and of the velocity of the phase change. In order to appreciate the advantage of the mathematical model adopted, we present in Fig. 4 also the numerical phase fronts obtained by "freezing" the solid mechanics: we notice that the plot in Fig. 2 is definitely much closer to the experimental than the last one. At first glance, looking at the unphysical bumps of the fronts in Fig. 4, one might be tempted to conclude that, when solid mechanics is not included in the model, the computed melt flow assumes an *undesired* multicellular structure, responsible of those shapes due to heat transfer.
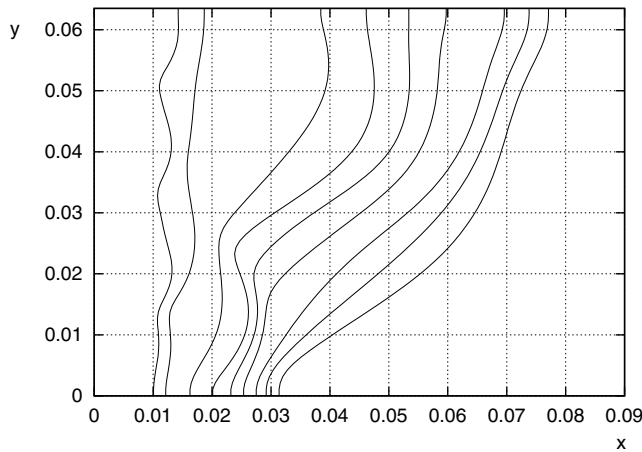

Figure 4. **Simulated** L/S phase fronts (solid mechanics *neglected* in the modeling) at the observation time instants of the experiment (m is the measure unit over (x) and (y) axes).

And one might extrapolate that the melt flow obtained from the complete model is unicellular. On the contrary, in both cases, as is shown by the melt flow streamlines at $t = 6$ min in Fig. 5 (solid mechanics included) and Fig. 6 (solid mechanics "frozen"), the computed melt flow is multicellular. This is possible as, within the complete model, the solid phase, through the stress developed at the interface and transferred to the melt, by virtue of the jump condition (2.8), locally counteracts the anomalous melting which carries the bumpy fronts even though the computed melt velocity is about 10 % larger when solid mechanics is included, consistently with the jump condition (2.7).

In comparison with other numerical simulations in literature, in our results the role of the viscous dissipation (see equation (2.3)) that is usually neglected, has to be recognized.
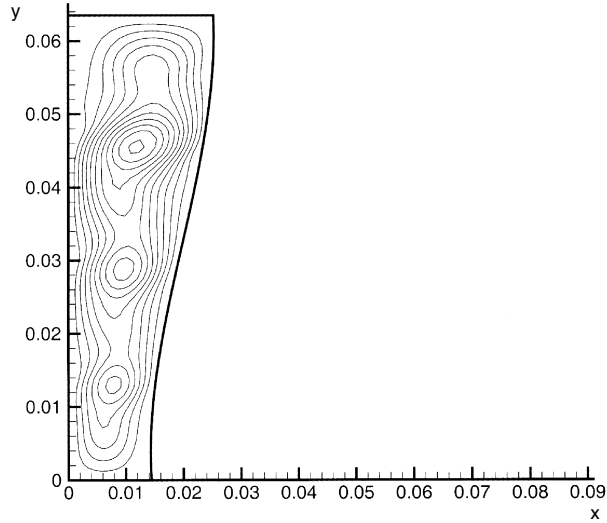
129

Figure 5. Melt flow streamlines (solid mechanics *included* in the modeling) at $t = 6$ min (m is the measure unit over (x) and (y) axes).
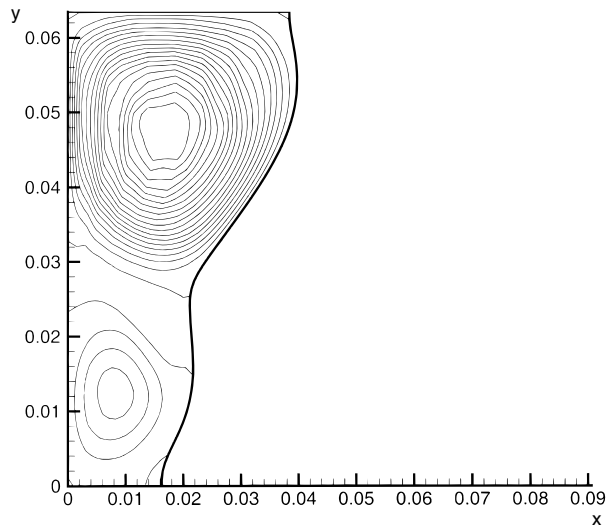

Figure 6. Melt flow streamlines (solid mechanics *neglected* in the modeling) at $t = 6$ min (m is the measure unit over (x) and (y) axes).

For the sake of completeness, we include in Fig. 7, Fig. 8 and Fig. 9 the vector plot of the displacement field of the solid phase computed respectively at $t = 1$ min, 8 min, and 19 min (appropriate magnifying factors have been used in order to make the plots readable). We stress that the typical oscillatory structure of a solution of a hyperbolic vector equation is caught; furthermore, the average modulus of displacement appears
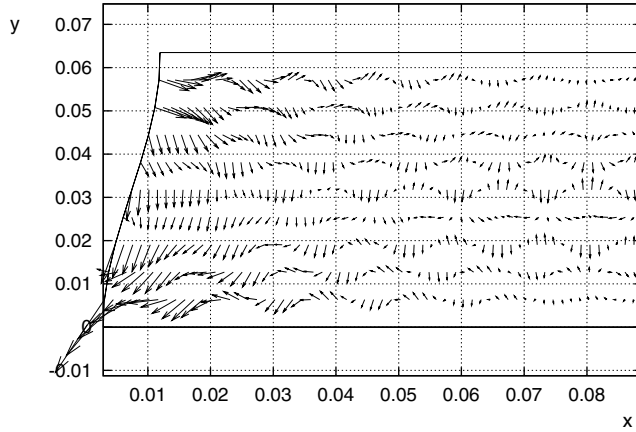
130

Figure 7. Simulated displacement field at $t = 1$ min (m is the measure unit over (x) and (y) axes, factor scale for the arrow length is 3000).
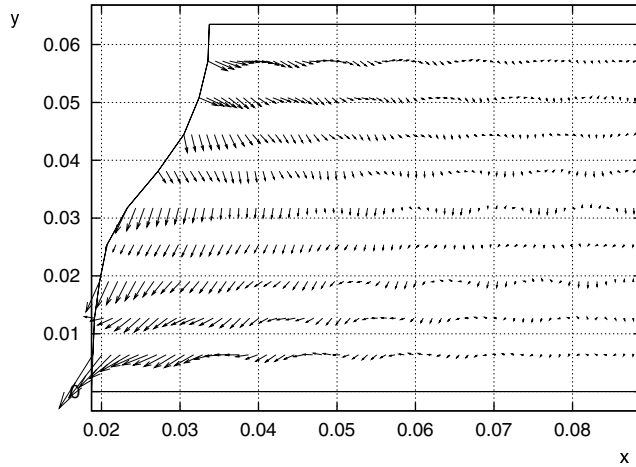

Figure 8. Simulated displacement field at $t = 8$ min (m is the measure unit over (x) and (y) axes, factor scale for the arrow length is 800).

increasing with time along with the increase of the average modulus of velocity of the convected melt. At time $t = 19$ min, the maximum modulus of the computed displacement vectors amounts to 0.5 mm.

6. CONCLUSIONS

The analysis of the past (till very recent) literature on the two-dimensional numerical simulation of this Gau & Viskanta experiment leads to the following significant considerations:
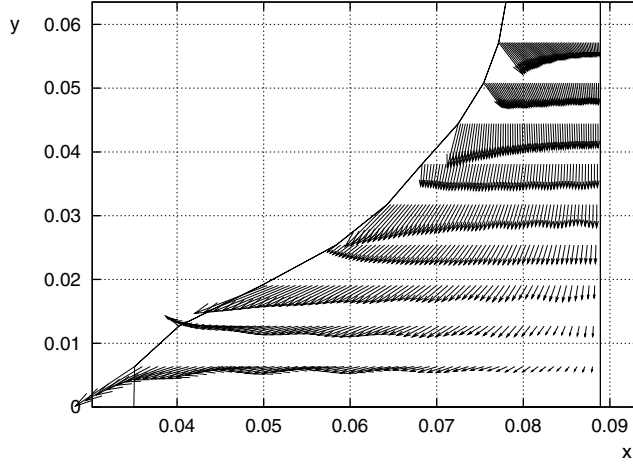
131

Figure 9. Simulated displacement field at $t = 19$ min (m is the measure unit over (x) and (y) axes, factor scale for the arrow length is 20).

   i) the multicellular flow structure of the melt convection meets expectations from
      fluid dynamics (Lee & Korpela [38], Derebail & Koster [17]), and from *ad hoc*
      stability analysis of melting from a side (Le Quere & Gobin [39]),
  ii) the multicellular flow structure of the melt convection appears combined with
      unphysical wavy shaped phase fronts (Dantzig [14], Stella & Giangi [48], Han-
      noun et al. [27]),
 iii) certain low order numerical schemes yield one main cell melt flow and produce
      smoother phase fronts, surprisingly closer to experimental observation (Brent
      et al. [6], Viswanath & Jaluria [55]),
  iv) some specialists, counting on highly accurate numerical discretizations, have
      started to explain the inconsistencies by conjecturing that the mathematical
      models in use for phase change with convection are not adequate for this exper-
      iment (Hannoun et al. [26], Tenchev et al. [51]).

It is worth mentioning that Cerimele et al. [7] gave a further interpretation to this
mismatching based on the observation that the sequence "stop and go" at each
measurement step of the experiment has never been properly reproduced and, by
simulating more carefully the procedure conducted by Gau & Viskanta, obtained
numerical results with melt flows still multicellular but slower, with a lower number
of cells and, consequently, with phase fronts with a lower number of bumps.

   Our simulation results successfully incorporate observation i) and iv) and definitely
embody neither the limitation ii) nor iii). Although in [26], even in the title of their
paper, Hannoun et al. claim to have resolved any controversy among the scientists
on this experiment, in fact they do not give any explicit suggestion for improving

132

the quality of the numerical simulations. Whereas, with the results presented in Section 5, we show that, just by including in the mathematical model the description of the mechanics of the solid phase, we reach a much more successful match with the Gau & Viskanta observation.

For the sake of completeness of this discussion, we want to refer also to the three-dimensional simulation developed by Kumar et al. [36] where the authors present multicellular convection flow of the melt as well as a good comparison with the evolving interface. This result, indeed published without mesh refinement analysis, is compatible with the presence of walls in the third direction as they weaken the melt convection rolls and consequent heat transfer, preventing the formation of a wavy shaped phase front. However, we recall again that, in our simulation, when solid mechanics is included, the opposite happens, that is, the solid phase slightly speeds up the melt convection due to the "pulling action" at the interface where solid particles are themselves under motion at the same velocity of the liquid phase particles; actually, the absence of bumps at the L/S interface is not at all due to an intuitive, though untrue, damping effect of the solid phase over the liquid phase but it is driven by the overall dynamical mechanisms in being. Moreover, on providing the two-dimensional plot of the interface in Fig. 3, Gau & Viskanta pointed out that the physical interface was "*smooth and flat in the direction perpendicular to the front and back walls of the test cell. This suggests that fluid motion and heat transfer in that direction was small, and the effect of natural convection recirculation on the interface motion can justifiably be neglected.*" Nevertheless, we are aware that two-dimensional modelling may introduce *a priori* a significant approximation of the overall real process but, in the present case, our results meet also the considerations from the experiment conducted by Costanza et al. [11] and Gondi et al. [25] who observed that solid phase dynamically interacts with melt during the phase transition process. Upon this convinction, we suggest the revision of the numerical simulations without the solid phase effects, in particular, the numerous applications to artificial crystal growth reported in the literature of the past thirty years and other ones where phase front shape represents a particularly critical aspect (e.g. Gadkari et al. [21], De Vahl Davis et al. [18]).

133

References

[1] *T. M. Apostol*: Calculus. Vol. II: Multi-variable calculus and linear algebra, with appli-
     cations to differential equations and probability. 2nd ed. Blaisdell Publishing Company,
     Waltham, 1969.

[2] *C. Bailey, P. Chow, M. Cross, Y. Freyer, K. Pericleous*: Multiphysics modelling of the
     metals casting process. Proc. R. Soc. Lond. A. *452* (1996), 459–486.

[3] *F. Baldoni*: Thermomechanics of Solidification. Pittsburgh University Press, Pittsburgh,
     1997.

[4] *E. Bansch, A. Smith*: Simulation of dendritic crystal growth in thermal convection.
     Interfaces and Free Boundaries *2* (2000), 95–115.

[5] *O. Bertrand, B. Binet, H. Combeau, S. Couturier, Y. Delannoy, D. Gobin, M. Lacroix,
     P. Le Quere, M. Medale, J. Mercinger, H. Sadat, G. Vieira*: Melting driven by natural
     convection. A comparison exercise: first results. Int. J. Therm. Sci. *38* (1999), 5–26.

[6] *A. D. Brent, V. R. Volle, K. J. Reid*: Enthalpy-porosity technique for modeling convec-
     tion-diffusion phase change: application to the melting of a pure metal. Numer. Heat
     Transfer *13* (1988), 297–318.

[7] *M. M. Cerimele, D. Mansutti, F. Pistella*: A front-fixing method for flows in liquid/solid
     phase change with a benchmark test. CD-Rom Proceedings of ECCOMAS 2000,
     Barcelona, September 11–14, 2000.

[8] *B. Chalmers*: Principles of Solidification. J. Wiley & Sons, New York, 1964.

[9] *P. Y. P. Chen, V. Timchenko, E. Leonardi, G. de Vahl Davis, H. C. de Groh III*: A
     numerical study of directional solidification and melting in microgravity. Proceedings
     of the ASME, Heat Transfer Division Vol. 3. 1998, pp. 75–83.

[10] *F. M. Chiesa, R. I. L. Guthie*: Natural convection heat transfer rate during the solidifi-
     cation and melting of metals and alloy systems. J. Heat Transfer *99* (1977), 520–526.

[11] *G. Costanza, F. Gauzzi, R. Montanari*: Structures of solid and liquid during melting
     and solidification of indium. Ann. New York Acad. Sci. *974* (2002), 68–78.

[12] *J. Crank*: Free and Moving Boundary Problems. Oxford Science Publication. Clarendon
     Press, Oxford, 1984.

[13] *M. Cross, C. Bailey, K. Pericleous, A. Williams, V. Bojarevics, N. Croft, G. Taylor*:
     The multiphysics modeling of solidification and melting processes. JOM-e *54* (2002).

[14] *J. Dantzig*: Modelling liquid-solid phase change with melt convection. Int. J. Numer.
     Methods Eng. *28* (1989), 1769–1785.

[15] *G. De Fabritiis, A. Mancini, D. Mansutti, S. Succi*: Mesoscopic models of liquid/solid
     phase transitions. Int. J. Modern Physics C. *9* (1998), 1405–1415.

[16] *H. C. de Groh III, T. Lindstrom*: Interface shape and convection during solidification
     and melting of succinonitrile. NASA Technical Memorandum 106487. 1994.

[17] *R. Derebail, J. N. Koster*: Numerical simulation of natural convection of gallium in a
     narrow gap. Int. J. Heat Mass Transfer *40* (1997), 1169–1180.

[18] *G. De Vahl Davis, K. Hanjalic, P. Le Quere, P. Bontoux, Eds.*: Progress in Computa-
     tional Heat and Mass Transfer. Proc 4th Int. Conf. Comput. Heat Mass Transfer, May
     17–20, 2005, Paris. Lavoisier, Paris, 2005.

[19] *P. G. Drazin, W. H. Reid*: Hydrodynamic Stability. Cambridge University Press, Cam-
     bridge, 1985.

[20] *M. Epstein, F. B. Cheung*: Complex freezing melting interfaces in fluid flow. Ann. Rev.
     Fluid Mech. *15* (1983), 293–319.

[21] *D. B. Gadkari, P. Shashidharan, K. B. Lal, B. M. Arora*: Influence of crystal-melt in-
     terface shape on self-seeding and single crystalline quality. Bull. Mater. Sci. *24* (2001),
     475–482.

134

[22] *C. Gau, R. Viskanta*: Melting and solidification of a metal system in a rectangular cavity. Int. J. Heat Mass Transfer *27* (1984), 113–123.

[23] *C. Gau, R. Viskanta*: Melting and solidification of a pure metal on a vertical wall. Transaction of the ASME *108* (1986), 174–181.

[24] *G. Golub, C. van Loan*: Matrix Computations. The Johns Hopkins University Press, Baltimore, 1989.

[25] *P. Gondi, R. Montanari, E. Evangelista, G. Buroni*: X-ray study of structures of liquid metals with controlled convective motions. Microgravity Quarterly *7* (1997), 155–173.

[26] *N. Hannoun, V. Alexiades, T. Z. Mai*: Resolving the controversy over tin and gallium melting in a rectangular cavity heated from the side. Numerical Heat Transfer, Part B *44* (2003), 253–276.

[27] *N. Hannoun, V. Alexiades, T. Z. Mai*: A reference solution for phase change with convection. Int. J. Numer. Methods Fluids *48* (2005), 1283–1308.

[28] *R. N. Hills, P. H. Roberts*: A macroscopic model of phase coarsening. Int. J. Non-Linear Mech. *25* (1990), 319–329.

[29] *G. J. Hirasaki, J. D. Hellums*: Boundary conditions on the vector and scalar potentials in viscous three-dimensional hydrodynamics. Q. Appl. Math. *28* (1970), 293–296.

[30] *A. Hoger, B. E. Johnson*: Linear elasticity for constrained materials: Incompressibility. J. Elasticity *38* (1995), 69–93.

[31] *S. C. Hunter*: Mechanics of Continuous Media. Ellis Horwood Limited, Chichester, 1976.

[32] *D. T. J. Hurle*: Convective transport in melt growth systems. J. Crystal Growth *65* (1983), 124–132.

[33] *H. E. Huppert*: The fluid mechanics of solidification. J Fluid Mech. *212* (1990), 209–240.

[34] *K. Kang, H. Ryou*: Computation of solidification and melting using the PISO algorithm. Numer. Heat Transfer, Part B *46* (2004), 179–194.

[35] *S. Kim, S. Anghaie, G. Chen*: Numerical prediction of multicellular melt flow during natural convection-dominated melting. J. Thermophysics and Heat Transfer *17* (2003), 62–68.

[36] *V. Kumar, F. Durst, S. Ray*: Modeling moving-boundary problems of solidification and melting adopting an arbitrary Lagragian-Eulerian approach. Numer. Heat Transfer, Part B *49* (2006), 299–331.

[37] *A. Lamazouade, M. El Ganaoui, D. Morvan, P. Bontoux*: Numerical simulation of thermo-solutal convection during Bridgman crystal growth. Revue Generale de Thermique *38* (1999), 674–683.

[38] *Y. Lee, S. A. Korpela*: Multicellular natural convection in a vertical slot. J. Fluid Mech. *126* (1983), 91–121.

[39] *P. Le Quere, D. Gobin*: A note on possible flow instabilities in melting from the side. Int. J. Thermal Sci. *38* (1999), 595–600.

[40] *D. Mansutti, G. Graziani, R. Piva*: A discrete vector potential model for unsteady incompressible viscous flows. J. Comput. Phys. *92* (1991), 161–184.

[41] *D. Mansutti, F. Baldoni, K. R. Rajagopal*: On the influence of the deformation of the forming solid in the solidification of a semi-infinte water-layer of fluid. Math. Models Methods Appl. Sci. *11* (2001), 367–386.

[42] *D. Mansutti, R. Raffo, R. Santi*: Liquid/Solid phase change with convection and deformations: 2D case. Progress in Industrial Mathematics at ECMI Mathematics in Industry Vol. 8, 2004 (A. Di Bucchianico, R. M. M. Mattheij, M. A. Peletier, eds.). Springer, Berlin, 2006, pp. 268–272.

[43] *W. Miller, S. Succi, D. Mansutti*: A lattice Boltzmann model for anisotropic liquid/solid phase transition. Phys. Rev. Lett. *86* (2001), 3578–3581.

[44] *M. A. Rady, A. K. Mohanty*: Natural convection during melting and solidification of pure metals in a cavity. Numer. Heat Transfer, Part A *29* (1996), 49–63.

[45] *R. Sampath, N. Zabaras*: An object oriented implementation of a front tracking finite element method for directional solidification processes. Int. J. Numer. Methods Eng. *44* (1999), 1227–1265.

[46] *J. C. Slattery*: Momentum, Energy and Mass Transfer in Continua. McGraw-Hill, New York, 1972.

[47] *R. Song, G. Dhatt, A. Ben Cheikh*: Thermo-mechanical finite element model of casting systems. Int. J. Numer. Methods Eng. *30* (1990), 579–599.

[48] *F. Stella, M. Giangi*: Melting of a pure metal on a vertical wall: numerical simulation. Numer. Heat Transfer, Part A *38* (2000), 193–208.

[49] *J. Stefan*: Über die Theorie der Eisbildung, insbesondere über die Eisbildung im Polarmeere. Sitzungsberichte der Österreichischen Akademie der Wissenschaften Mathematisch-Naturwissen-schaftliche Klasse, Abteilung 2, Mathematik, Astronomie, Physik, Meteorologie und Technik *98* (1988), 965–983. (In German.)

[50] *J. Szekely, P. S. Chambra*: The effect of natural convection on the shape and movement of the melt-solid interface in the controlled solidification. Met. Trans. B1 (1970), 1195–1203.

[51] *R. T. Tenchev, J. A. Mackenzie, T. J. Scanlon, M. T. Stickland*: Finite element moving mesh analysis of phase change problems with natural convection. Int. J. Heat Fluid Flow *26* (2005), 597–612.

[52] *A. Teskeredzic, I. Demirdzic, S. Muzaferija*: Numerical method for heat transfer, fluid flow and stress analysis in phase-change problems. Numer. Heat Transfer, Part B *42* (2002), 437–459.

[53] *C. Truesdell, K. R. Rajagopal*: An Introduction to the Mechanics of Fluids. Birkhäuser, Boston, 2000.

[54] *H. Van der Vorst*: Bi-CGSTAB: A fast and smoothly converging variant of the Bi-CG for the solution of non-symmetric linear systems. SIAM J. Sci. Stat. Comput. *13* (1992), 631–644.

[55] *R. Viswanath, Y. Jaluria*: A comparison of different solution methodologies for melting and solidification problems in enclosures. Numer. Heat Transfer, Part B. *24* (1993), 77–105.

[56] *V. R. Voller, M. Cross, N. Markatos*: An enthalpy method for convection/diffusion phase change. Int. J. Numer. Methods Eng. *24* (1987), 271–284.

[57] *V. R. Voller*: An overview of numerical methods for solving phase change problems: a review. Adv. Numer. Heat Transfer (W. J. Minkowycz, E. M. Sparrow, eds.). Taylor & Francis, Philadelphia, 1997.

[58] *G. H. Yeoh, G. de Vahl Davis, E. Leonardi, H. C. de Groh III, M. Yao*: A numerical and experimental study of natural convection and interface shape in crystal growth. J. Crystal Growth *173* (1997), 492–502.

Authors' addresses: *D. Mansutti*, Istituto per le Applicazioni del Calcolo/C.N.R., Via dei Taurini, 19, 00186 Roma, Italy, e-mail: `d.mansutti@iac.cnr.it`; *E. Bucchignani*, Centro Italiano Ricerche Aerospaziali, Via Maiorise, 81043 Capua (CE), Italy, e-mail: `e.bucchignani@cira.it`.

www.manaraa.com